



**A MULTIPLE DESIGN POINT OPTIMIZATION OF
HIGH SPEED PROPROPOTORS**

BY

ADITI CHATTOPADHYAY, THOMAS R. MCCARTHY AND CHARLES E. SEELEY

DEPARTMENT OF MECHANICAL AND AEROSPACE ENGINEERING
ARIZONA STATE UNIVERSITY
TEMPE, ARIZONA 85287-6106

TWENTIETH EUROPEAN ROTORCRAFT FORUM
OCTOBER 4 - 7, 1994 AMSTERDAM

A MULTIPLE DESIGN POINT OPTIMIZATION OF HIGH SPEED PROPRATORS

Aditi Chattopadhyay[†], Thomas R. McCarthy[‡] and Charles E. Seeley[‡]
Department of Mechanical and Aerospace Engineering
Arizona State University
Tempe, Arizona 85287-6106

1. ABSTRACT

A multipoint optimization procedure is developed to investigate design trade-offs in high speed tilting proprotor aircraft. The design points include high speed cruise, take-off and hover. A multilevel decomposition scheme is used in the optimization with aerodynamic and structural performance as the objectives and constraints in the upper and lower levels, respectively. A multiobjective optimization procedure is used to formulate the problem at each level. The optimization problem consists of a nonlinear programming technique at the upper level and a discrete procedure based on the simulated annealing algorithm at the lower level. The effect of composite tailoring on rotor aerodynamic performance is investigated by modeling a composite box beam to represent the principal load carrying member in the rotor. The aerodynamic analysis is performed using the classical blade element momentum approach which includes a representation of the high lift potential of propeller/rotor blades in comparison to two dimensional airfoil properties. The structural analysis is performed using a quasi-one dimensional finite element model based on an analytical composite box beam representation. Optimum designs are compared with an existing rotor blade performance which is used as a baseline or reference design. The results show significant improvements in both the aerodynamic and structural performance at all design points.

2. NOMENCLATURE

c	chord, ft
c_d	coefficient of drag
c_l	coefficient of lift
g_j	constraint function vector
k_{ij}	stiffness matrix, p.s.i.
r	radial location, ft
t	wall thickness, in
r_c	simulated annealing cooling rate
t/c	thickness to chord ratio
u_T	swirl velocity, ft/s
u, v, w	elastic displacements
x, y, z	reference axes
F	axial force (lb)
F_k	objective functions
F_{k0}	values of F_k at the beginning of an iteration
FM	hover figure of merit
M_y	flapping moment, lb-in
M_z	lagging moment, lb-in
NC	number of constraints
NDV	number of design variables
NF	number of objective functions
NSEG	number of blade segments
P	random number, $0 < P < 1$
P_{acc}	acceptance probability
Q	blade torque, lb-ft

[†] Associate Professor, Senior Member AIAA, Member AHS, ASME, SPIE, ISSMO, AAM

[‡] Graduate Research Assistant, Member AHS, AIAA

Q_y	transverse horizontal shear force, lb
Q_z	transverse vertical shear force, lb
R	blade radius, ft
T	thrust, lb
T_k	simulated annealing "temperature"
V	forward velocity, ft/s
W	total local blade velocity, ft/s
α	local blade angle of attack
α_{zl}	zero lift angle, deg.
ϕ	elastic twist
$\gamma_{\chi\eta}, \gamma_{\chi\zeta}$	shear strains
κ	box beam scaling factor
η, ζ	local blade element axes
η_c	rotor propulsive efficiency
θ	blade twist, degrees
ρ	K-S function multiplier
σ_1, σ_2	material axis normal stresses, p.s.i.
τ_{12}	shear stress, p.s.i.
v_i	induced velocity, ft/s
Λ	blade sweep, degrees
Φ	design variable vector
Ω	rotor angular velocity, r.p.m.

3. INTRODUCTION

Tilt rotor aircraft, which combines the take-off and hover capabilities of helicopters with cruise performance of fixed-wing aircraft have been of interest recently¹⁻³. There are several conflicting requirements associated with these design goals. For example, efficient cruise performance requires thin blade sections which compromise hover performance. Blade sweep, which can help reduce high tip Mach numbers (M_{tip}), thereby improving high speed efficiency, can also adversely affect the structural performance.

Recently, research efforts have been initiated by Chattopadhyay et al.⁴⁻¹⁰ to develop formal optimization procedures for addressing these issues in the design of tilt rotor aircraft. In Refs. 4 and 5 optimization procedures were developed to maximize high speed cruise propulsive efficiency without degrading hover figure of merit. An optimization procedure was developed in Ref. 6 to address the problem of aeroelastic stability in high speed cruise. In Ref. 7, the drive system weight was minimized and the associated trade-offs in cruise efficiency were investigated. The integrated aerodynamic, aeroelastic and structural optimization problem was addressed in Ref. 8. McCarthy et al.⁹ developed a purely aerodynamic multiobjective optimization procedure for improved high speed cruise and hovering performance using planform and airfoil characteristics as design variables. More recently, Chattopadhyay et al.¹⁰ developed a multilevel decomposition based optimization procedure in which the goal was to improve aerodynamic performance in hover and cruise in the upper level and to improve structural characteristics, in these flight modes, at the lower level. The results presented in Refs. 9 and 10 were obtained by using a simple aerodynamic code based on blade element approach and two dimensional airfoil theories. These were later corroborated by Dadone et al.¹¹ in a parametric study conducted to investigate the important design issues associated with the development of high speed proprotors using a comprehensive Euler analysis. This study extends the work of Ref.10 by including take-off performance in the optimization formulation. The aerodynamic and structural design criteria in high speed cruise, in hover and

in take-off are addressed using a multilevel decomposition based optimization procedure. At the upper level, the aerodynamic performance of proprotors is optimized for each flight condition using planform variables. Constraints are imposed on the rotor thrust in all three flight conditions. A nonlinear programming technique based on the Broyden-Fletcher-Goldfarb-Shanno (BFGS) algorithm is used for the optimization. At the lower level, the rotor is optimized for improved structural performance using composite ply stacking sequence as design variables. Since only discrete design variables are used at the lower level, an optimization procedure, based on simulated annealing algorithm¹², is developed to address this complex problem. The results of the optimization procedure are compared with an existing rotor¹³.

4. ANALYSIS

For the aerodynamics analysis, an algorithm based on blade element momentum approach is used. The procedure offers a significant reduction in computational effort from more comprehensive procedures which were previously used by Chattopadhyay and McCarthy⁴⁻⁸ in the analysis of tilt rotor aircraft. The use of this analysis within an optimization procedure also provides realistic design trends which can be verified by comparing the results obtained by McCarthy et al.^{9,10} with those obtained using an Euler code by Dadone et al.¹¹.

The structural analysis is performed using a composite box beam model which includes blade pre-twist, taper and sweep to represent the principal load carrying member in the blade. The semi-analytical technique used in this study, which is an extension of the quasi one-dimensional beam developed by Smith and Chopra¹⁴, offers significant computational savings from more refined finite element models while maintaining sufficient accuracy.

4.1 Aerodynamic Analysis

The aerodynamic formulation is based on blade element approach initially developed by Smith¹⁵ and later modified by Talbot¹⁶. In this approach, the two dimensional aspects of rotorcraft airfoils are modeled more accurately than the traditional 2-D airfoil theory to include the effects of stall delay due to the rotation of the blade. Further, analytical closed form expressions are available for the calculation of aerodynamic performance in terms of variables such as planform, camber and thickness. This allows for variations of these parameters during optimization for complete investigation of their effects on aerodynamic performance. The blade element theory used in the algorithm is due to Glauert¹⁷. An empirical fit was performed on NACA 63 and 64 series airfoil families in order to supply a functional relationship between maximum lift coefficient and the sectional thickness and camber for incompressible flow. The theory calculates a blade element force based on two equations: the force due to the sectional coefficients of lift (c_l) and drag (c_d) and the force due to the change in momentum of air passing through an annulus swept by the blade element as follows.

$$dT_1 = 4\pi r \rho (V + v_i) v_i dr \quad (1)$$

$$dT_2 = \frac{1}{2} \rho W^2 c (c_l \cos \alpha - c_d \sin \alpha) dr \quad (2)$$

$$dQ_1 = 4\pi r^2 \rho (V + v_i) u_T dr \quad (3)$$

$$dQ_2 = \frac{1}{2} \rho W^2 c (c_l \sin \alpha + c_d \cos \alpha) r dr \quad (4)$$

where dT , dQ and dr represent the section thrust, torque and element length, respectively, W is magnitude of the resultant velocity, V is the forward velocity and v_i and u_T represent the inflow and swirl velocities, respectively. The chord length and radial location are denoted c and r , respectively, ρ is the density of air and α is the local angle of attack of the blade section. This system of equations is then used to solve for the inflow and swirl velocities by equating the thrusts and the torques.

The algorithm has been found to correlate extremely well with advanced technology blades and the procedure also yields meaningful design trends when used in formal optimization procedures^{9,10}. This code has been further modified by the authors to allow spanwise variation of sweep to investigate the effect of sweep as a design variable. The aerodynamic analysis is coupled with the structural analysis procedure which is described next. The results of the complete analysis represent trimmed static solutions which include the effects of elastic deformations.

4.2 Structural Analysis

The load carrying member of the rotor is modeled as a single-celled composite box beam (Fig. 1). However, the weights of the honeycomb structure and the blade skin are also included in the total weight calculation. The blade is discretized using finite elements with 19 total degrees of freedom, U_e , and unequal element sizes. The nodal degrees of freedom are described as follows.

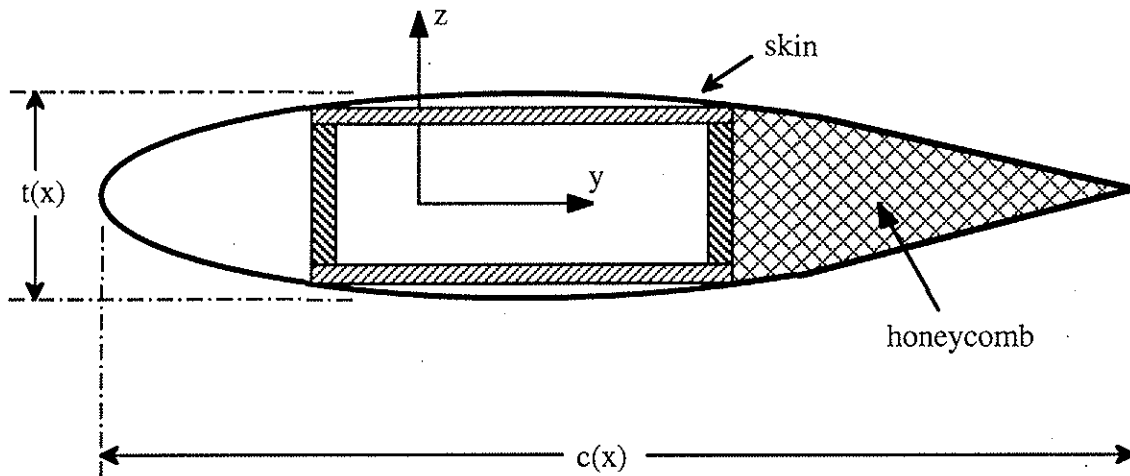


Figure 1 Blade cross section

$$U_e^T = [u_1, u_2, u_3, u_4, v_{b1}, v'_{b1}, v_{b2}, v'_{b2}, w_{b1}, w'_{b1}, w_{b2}, w'_{b2}, \phi_1, \phi_2, \phi_3, v_{s1}, v_{s2}, w_{s1}, w_{s2}] \quad (5)$$

where u is the axial displacement, v and w are the inplane horizontal and vertical displacements and ϕ is the elastic twist. First partial derivatives with respect to the spanwise axis (x) are denoted ($'$). The formulation assumes that the inplane displacements can be decoupled into a term corresponding to pure bending and a term corresponding to shear as shown below.

$$v = v_b + v_s \quad (6)$$

$$w = w_b + w_s \quad (7)$$

where the subscripts (b) and (s) refer to bending and shear displacements, respectively. Identical node locations are used in specifying both aerodynamic and structural parameters.

The outer dimensions of the box beam (Fig. 2) are constant percentages of the chord and thickness. Each composite plate used to model the composite box beam is assumed to be symmetric about the midplane of the plate and is made up of 24 laminated orthotropic composite plies. Further, the box beam is assumed to have double symmetry about the local coordinate axes (η and ζ). This ensures that the two vertical walls are identical to each other and also that the two horizontal walls are identical. The vertical and horizontal walls, however, are assumed to be independent of each other. The beam cross section is described by stretching, bending, twisting, shearing and torsion related warping and is an extension of a

modeled developed by Smith and Chopra¹⁴. Based on this model, the equations of equilibrium are written as follows.

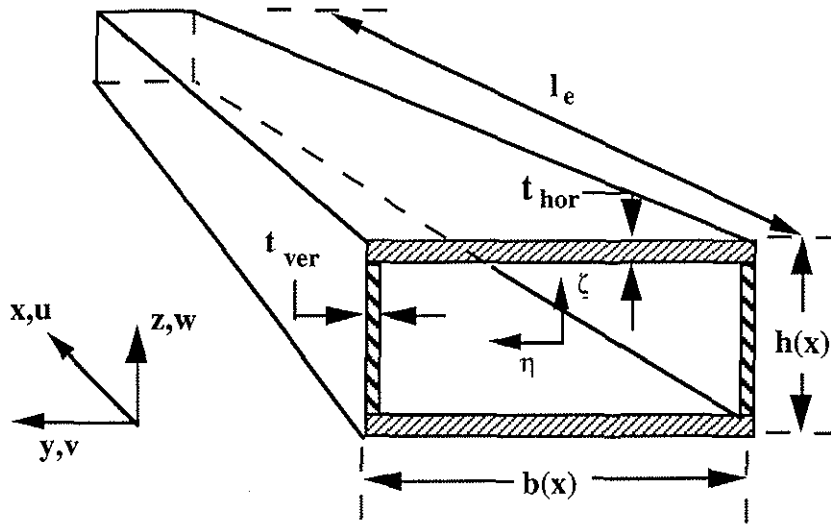


Figure 2 Composite box beam

$$\begin{Bmatrix} F \\ Q_y \\ Q_z \end{Bmatrix} = \begin{bmatrix} k_{11} & 0 & k_{13} \\ 0 & k_{22} & k_{23} \\ k_{13} & k_{23} & k_{33} \end{bmatrix} \begin{Bmatrix} u' \\ \gamma_{x\eta}^o \\ \gamma_{x\zeta}^o \end{Bmatrix} \quad (8)$$

$$\begin{Bmatrix} T \\ M_y \\ M_z \end{Bmatrix} = \begin{bmatrix} k_{44} & 0 & k_{46} \\ 0 & k_{55} & k_{56} \\ k_{46} & k_{56} & k_{66} \end{bmatrix} \begin{Bmatrix} \phi' \\ w'' - \gamma_{x\zeta}^o \\ v'' - \gamma_{x\eta}^o \end{Bmatrix} \quad (9)$$

where M_z and M_y are the lagging and flapping moments, respectively, and T is the torsional moment. The axial force is denoted F , the inplane horizontal and vertical shear forces are denoted Q_y and Q_z , respectively and k_{ij} ($i, j = 1, 2, \dots, 6$) represent the stiffness matrix elements. The quantities $\gamma_{x\eta}^o$ and $\gamma_{x\zeta}^o$ represent inplane shear strains. The elemental equilibrium equations are written in vector form as follows.

$$\mathbf{F}_e = \mathbf{K}_e \mathbf{u}_e \quad (10)$$

where $\mathbf{F}_e = [F \ Q_y \ Q_z \ T \ m_x \ m_z]^T$ is the elemental force vector, $\mathbf{K}_e = [k_{ij}]$ is the elemental stiffness matrix and $\mathbf{u}_e = [u' \ \gamma_{x\eta}^o \ \gamma_{x\zeta}^o \ \phi' \ (v'' - \gamma_{x\eta}^o) \ (w'' - \gamma_{x\zeta}^o)]^T$ represents the elemental degrees of freedom in the local coordinate system. Using these principles and the nodal degrees of freedom, as described in Eqn 5, a finite element approach is developed using the weak formulation¹⁰.

5. OPTIMIZATION PROBLEM

The primary objectives are to improve aerodynamic and structural performance of the tilt rotor aircraft at three design points, high speed cruise, hover and take-off. Since the problem is complex and is associated with several objectives functions, constraints and design variables, a multilevel decomposition technique is used to decompose the problem into two levels. Such techniques have found application in fixed wing aircraft and recently have been used in helicopter design problems as well^{18,19}. More recently, Chattopadhyay et al. developed a two

level optimization procedure for the design of high speed propellers to maximize high speed cruise and hover performance simultaneously¹⁰. In this paper, the decomposition technique developed in Ref. 10 is used to formulate an optimization problem involving a total of three flight conditions. The optimization procedure is decomposed into two levels. The aerodynamic performance is improved at the upper level and the structural criteria are addressed at the lower level. The upper and lower levels are coupled through the use of optimal sensitivity parameters¹⁹, which are essential in maintaining proper coupling between the levels. Following is a description of the two levels.

5.1 Upper Level

The axial efficiency in high speed cruise (η_c) and the figure of merit in both hover and in take-off (FM_h and FM_t , respectively) are maximized simultaneously in this level using aerodynamic design variables. Constraints are imposed on the rotor thrust at each of these flight conditions. Geometric constraints are also imposed on the physical dimensions of the blade to ensure that the load carrying member of the rotor is maintained within the dimensions of the airfoil. The blade is discretized and design variables include the values of chord (c), twist (θ), thickness to chord ratio (t/c) and zero lift angle of attack (α_{z1}) at each node. To ensure monotony of the sweep, the following quadratic variation is used to represent the lifting line.

$$y_{a/c} = \frac{1}{2} d_1 x^2 \quad (11)$$

where $y_{a/c}$ is the position of the aerodynamic center, which in this formulation coincides with the shear center. The coefficient d_1 is used as a design variable to determine this position. The sweep distribution can then be formulated using this expression as follows.

$$\Lambda(x) = \tan^{-1}(d_1 x) \quad (12)$$

This also ensure continuity of the elastic axis. The optimization problem is stated as follows.

Maximize

$$\eta_c(\Phi), FM_h(\Phi), FM_t(\Phi)$$

subject to

$$T_c = (T_c)_{ref}$$

$$T_h = (T_h)_{ref}$$

$$T_t = (T_t)_{ref}$$

$$\kappa t_{hor} \leq t_{max}$$

where $\Phi = [c(x), \theta(x), \Lambda(x), \alpha_{z1}(x), t/c(x)]$ is the design variable vector, the subscripts 'c', 'h' and 't' refer to cruise, hover and take-off conditions, respectively and the subscript 'ref' indicates reference rotor value. The quantity t_{hor} is the thickness of the horizontal wall in the box beam, t_{max} is the maximum thickness of the airfoil and κ is a scaling factor used to ensure that the box beam is maintained within the airfoil cross section.

5.2 Lower Level

The structural characteristics of the rotor are investigated at this level. The objectives are to minimize the tip displacements in cruise, in hover and in take-off. The most critical of these displacements are included in the formulation. In cruise, the elastic twist (ϕ_c) and the inplane displacement (v_c) are critical. In hover and in take-off conditions, the vertical displacement (w_h and w_t , respectively) and the elastic twist (ϕ_h and ϕ_t , respectively) are significant. Therefore, these six displacements are selected as the individual objective functions to be minimized. Ply orientations are used as design variables. However, to avoid impractical values, the ply angles

are chosen from a set of pre-selected values $[0^\circ, \pm 15^\circ, \pm 30^\circ, \dots, 90^\circ]$. Stress constraints are imposed and the Tsai-Wu failure criterion²⁰, which assumes the following form is used to reduce the number of these constraints.

$$\left(\frac{1}{\sigma_{1T}} - \frac{1}{\sigma_{1C}}\right)\sigma_1 + \left(\frac{1}{\sigma_{2T}} - \frac{1}{\sigma_{2C}}\right)\sigma_2 + \frac{\sigma_1^2}{\sigma_{1T}\sigma_{1C}} - \frac{\sigma_1\sigma_2}{\sqrt{\sigma_{1T}\sigma_{1C}\sigma_{2T}\sigma_{2C}}} + \frac{\sigma_2^2}{\sigma_{2T}\sigma_{2C}} + \frac{\tau_{12}^2}{\tau_{12S}^2} < 0 \quad (13)$$

where σ_1 and σ_2 represent normal stresses along the material axes and τ_{12} represents the shear stress (see Fig. 3). The subscripts 'T', 'C' and 'S' represent the ultimate stress in tension, in compression and in shear, respectively. Each of the composite plates used in the box beam modeling are assumed to be symmetric about the midplane of the plate and the beam itself is assumed to be symmetric about its local axes, η and ζ (Fig. 2). Therefore, the above failure criterion is imposed, on each lamina, at each of the four corners of the box beam to prevent failure due to stresses.

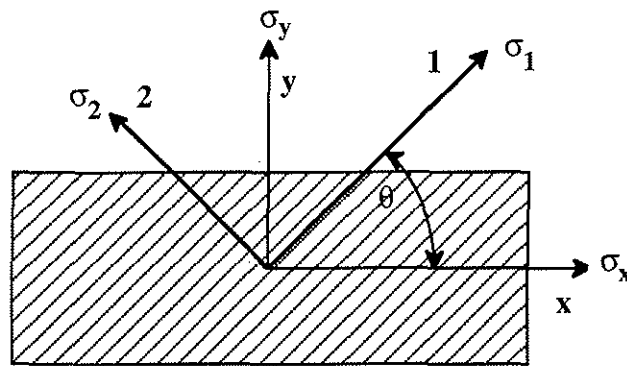


Figure 2 Composite lamina material axes

6. OPTIMIZATION IMPLEMENTATION

Standard optimization techniques are associated with a single objective function which can be minimized or maximized. Since the optimization problem addressed here involves multiple design objectives, the objective function formulation is more complicated. Often, the individual objective functions are combined using weight factors in a linear fashion¹⁸. Such methods are judgmental as the answer depends upon the weight factors which are often hard to justify. Therefore, the problem is formulated using the Kreisselmeier-Steinhauser (K-S) function approach²¹. Using this approach the multiple objective functions and the constraints are transformed into a single envelope function which is then extremized. The problem thus reduces to an unconstrained optimization problem. The K-S function technique has been found to perform very well in rotary wing applications^{6-10,19}

Since only continuous design variables are used during optimization at the upper level, a nonlinear programming procedure (NLP) based on the Broyden-Fletcher-Goldfarb-Shanno (BFGS) algorithm²² is used. The lower level comprises only discrete design variables, therefore an optimization technique based on the simulated annealing algorithm is implemented at this level. Since the objective functions and constraints must be evaluated several times before convergence is achieved, calculation of these values using exact analyses at each iteration is computationally prohibitive. Therefore, at the upper level, the objective functions and constraints are approximated using a two-point exponential expansion technique²³, which has been found to perform well in nonlinear optimization problems^{5-8,10,19}. This technique

takes its name from the fact that the exponent used in the expansion is based upon gradient information from the previous and current design cycles.

In order to ensure the validity of the approximation it is necessary to impose bounds, or “move limits” on the design variables during the optimization so that the design point remains in the neighborhood of the original point. These move limits represent a percent change from the original design variable. The move limits in this study are calculated using a variable scheme developed by Thomas et al.²⁴

If ply angles are modeled as continuous design variables and are later rounded off to the nearest practical value (e.g. 17.3° being rounded off to 18°), the result can lead to sub optimal designs²⁵. A more efficient technique is to allow the ply angles to vary within a set of prescribed values. Therefore, in the structural optimization problem at the lower level the goal is to determine the optimal stacking sequence from within a set of laminates which are integer multiples of 15° such as 0°, ±15°, ±30°, ..., 90°. This reduces the problem to a discrete optimization problem and conventional techniques are no longer applicable. Therefore, a procedure based on the simulated annealing algorithm is developed to address the completely discrete problem¹². The procedure is outlined below.

```

START
Current design is F
Perturb current design Fnew
If Fnew ≤ F then
    F = Fnew
Else if Pacc ≥ P then
    F = Fnew
End if
Go to START

```

where F is the objective function to be minimized and P is a random number such that $0 \leq P \leq 1$. The acceptance probability P_{acc} of retaining a worse design is computed as follows.

$$P_{acc} = \exp\left(-\frac{\Delta F}{T_k}\right) \quad (14)$$

where ΔF is the change in the objective function and T_k is the “temperature” which is reduced during successive iterations, to ensure smooth convergence, using the following relation.

$$T_k = (r_c)^k T_0 \quad (15)$$

where T_0 is the initial temperature and r_c is the cooling rate which determines the temperature at the k^{th} iteration. This reduces the probability of accepting a worse design. Occasionally accepting a worse design under the given probability allows the algorithm to climb out of possible local minima. The above loop is repeated a prescribed number of times for each cycle in the multilevel optimization procedure.

7. RESULTS

The reference rotor used is an existing advanced three-bladed gimballed rotor¹³. The aerodynamic optimization in high speed cruise is performed at a cruise altitude of 25,000 feet and a forward velocity of 300 knots with a rotational speed of 421 RPM. A vehicle weight of 13,000 lbs and aircraft lift to drag ratio (L/D) of 8.4 is assumed. Therefore, the thrust in cruise is constrained to be 774 lbs for the two engine aircraft. In hover, the aircraft is assumed to be operating at sea level conditions with a rotational speed of 570 RPM and a 12 percent down load effect from the rotor/wing interaction. The thrust in hover is therefore constrained to be at

7280 lbs. To simulate the take-off condition a load factor of 1.25 is used. Inclusion of the 12 percent down load effect, results in a take-off thrust of 9100 lbs. A rotational speed of 570 RPM is used and an altitude of 6695 feet is assumed to simulate a high altitude take-off. The operating conditions are summarized in Table 1. The blade is discretized into 10 segments. The composite material used in the structural analysis is carbon-PEEK AS4/APC2 which has properties as listed in Table 2.

Table 1. Summary of flight conditions

Vehicle weight	13,000 lb
Blade radius	12.5
Hover	
Altitude	Sea level
Thrust, T_h	7280 lb
Rotational speed	570 RPM
Cruise	
Altitude	25,000 ft
Thrust, T_c	774 lb
Rotational speed	421 RPM
Forward speed, V_∞	300 knots
Take-off	
Altitude	6695 ft
Thrust, T_t	9100 lb
Rotational speed	570 RPM

Table 2 Composite properties

Carbon-PEEK AS4/APC2		
E_1	19.43 (10^6)	p.s.i.
E_2	1.29 (10^6)	p.s.i.
G_{12}	0.74 (10^6)	p.s.i.
ν_{12}	0.28	
σ_{1T}	309. (10^3)	p.s.i.
σ_{1C}	160. (10^3)	p.s.i.
σ_{2T}	11.6 (10^3)	p.s.i.
σ_{2C}	29.0 (10^3)	p.s.i.
τ_{12s}	23.2 (10^3)	p.s.i.

At the upper level the design variables include the nodal values of the chord (c), twist (θ), zero angle of attack (α_{z1}) and thickness to chord ratio (t/c). The sweep distribution (Λ) is based on a quadratic lifting line. This yields a total of 45 design variables. The scaling factor (κ), used in the upper level constraints to ensure that the box beam is maintained within the airfoil section, is assumed to vary along the span as follows.

$$\kappa = \begin{cases} 4 & x < 0.7 \\ 3 & 0.7 \leq x < 0.9 \\ 2.5 & 0.9 \leq x \leq 1.0 \end{cases} \quad (16)$$

This also ensures the validity of thin wall theory at inboard sections of the blade, which carry the majority of the load, without being too restrictive at the tip where thinner airfoils can improve the aerodynamic performance. The tolerance on the lower level objective functions, used as optimal sensitivity parameters at this level, is initially set at 5 percent and is later relaxed to 20 percent for the tip bending displacements. An inhouse code based on the Kreisselmeier-Steinhauser (K-S) function developed at Arizona State University is used as the optimization algorithm at this level. The search direction used during optimization is based on the BFGS algorithm²¹ and the two-point exponential expansion is used to approximate the objective functions and constraints. The K-S function multiplier ρ is initially set at 50 and increases during optimization to values as high as 210.

At the lower level, the design variables used represent discrete values of the composite ply orientations. Since a symmetric and balanced lay-up is assumed in both the vertical and the horizontal walls, this leads to 12 independent design variables which can assume any one of the 7 pre-selected values of ply angle orientations. A value of 5 is used for ρ , the K-S function multiplier. In the simulated annealing algorithm a value of 0.995 is used for the cooling rate, r_c , and the initial temperature (T_0) is set to 1.0.

In the multilevel problem, a total of 150 cycles is necessary for convergence at the upper level where a cycle consists a "converged" design based upon one real analysis and several approximate function evaluations. A total of 5000 iterations are necessary at the lower level. Total convergence, including upper and lower levels, is achieved in five cycles. The results from this multiple design point optimization are presented in Tables 3 and 4 and Figs. 4 - 14.

The upper level objective functions are presented in Table 3 and Fig. 4. The figures of merit in hover (FM_h) and in take-off (FM_t) are increased by 6.9 and 31 percent, respectively, from the reference values. A small increase (0.52%) is obtained in the cruise propulsive efficiency (η_c). These trends can be explained by examining the rotor planform.

A comparison of the optimum and reference chord distributions (c) are shown in Fig. 5 and significant differences must be noted. The optimum distribution closely resembles the well known ideal hover planform with notable exceptions at the root and at the tip. The closeness to the hover planform is due to the large solidity necessary to achieve the thrust required in both hover and in take-off. The deviation (from ideal hover planform) at the root is a result of an upper bound of 0.2 which is imposed on the nondimensional chord (c/R) to avoid large chord sections. The deviation at the tip is due to a geometric constraint which is imposed to ensure that the box beam is maintained within the airfoil section. The reduction in the outboard section, relative to the reference rotor, is attributable to the lack of any maneuver margin requirement in the optimization problem formulation. Further, it is of interest to note that although the area-weighted solidity (σ) is increased by nearly 31 percent, the thrust weighted solidity (σ_T) is increased by only 7.1 percent (Table 3).

Table 3 Summary of optimum results

	Reference	Optimum
Objective functions		
Level 1:		
FM (hover)	0.760	0.813
$\eta_{\alpha x}$	0.888	0.893
FM (take-off)	0.617	0.807
Level 2		
w_h (in)	11.5	6.95
v_c (in)	-2.21	-1.03
w_t (in)	13.7	7.91
ϕ_h (deg)	-2.05	-1.77
ϕ_c (deg)	-1.22	-1.19
ϕ_t (deg)	-1.73	-1.39
Solidity		
area weighted, σ	0.08075	0.1055
thrust weighted, σ_t	0.08913	0.08976

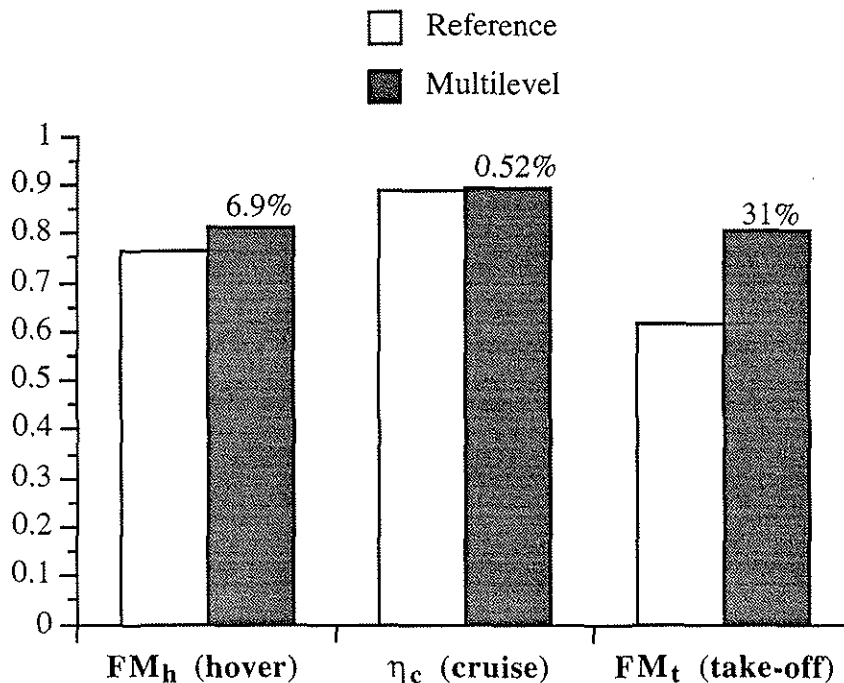


Figure 4 Summary of upper level objective functions

The thickness to chord ratio (t/c) distributions of the reference and the optimum rotor configurations are presented in Fig. 6 and show large reductions from the reference rotor at the inboard sections of the optimum rotor. The thickness is also slightly reduced from the reference values at midspan locations and is slightly increased at the tip. The former is explained as an attempt to improve the rotor performance by reducing the profile drag. The latter represents the optimizer's effort to satisfy the geometric constraint which ensures that the

box beam is contained within the airfoil section. Since the optimum distribution is very similar to the reference distribution at midspan locations and slight increases are observed at the tip, the profile drag over the working section of the blade in case of high speed cruise is only slightly altered. This, coupled with the chord distribution over this section of the blade, results in only a slight improvement of the high speed cruise propulsive efficiency (η_c).

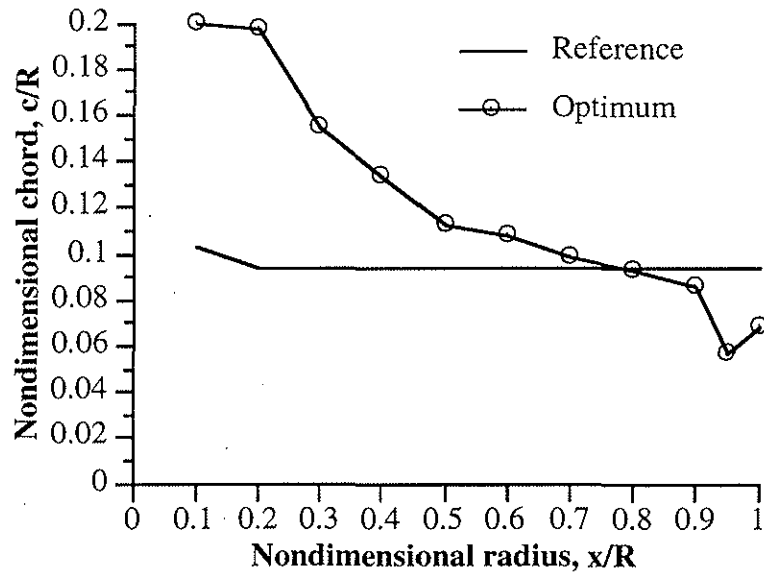


Figure 5 Chord distributions

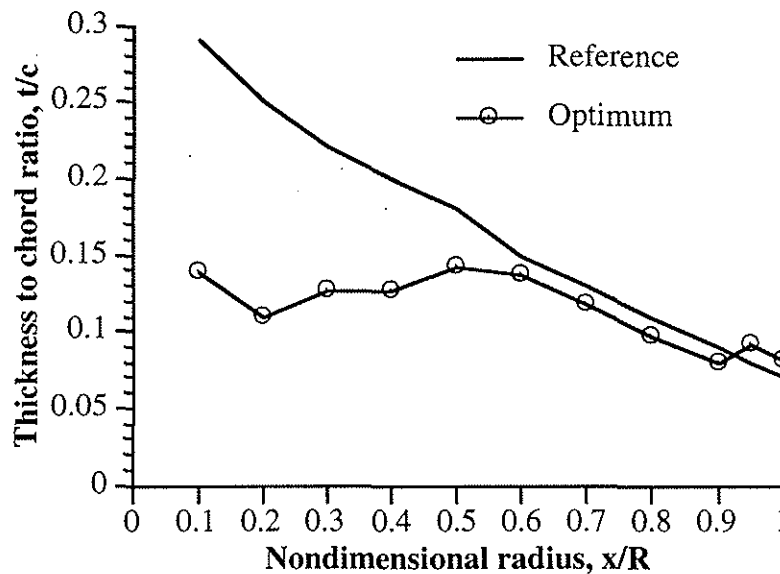


Figure 6 Thickness to chord ratio distributions

The twist distributions (θ) are presented in Fig. 7. The twist is reduced from reference to optimum values over the inboard section of the blade and is increased over the midspan section. At the outboard section of the blade, the twist remains almost unchanged after optimization. It must be noted from Fig. 7 that the largest differences between reference and optimum, in both inboard and midspan locations, is of the order of two degrees. However, the increase is achieved in a region of the blade which has greater resultant velocities. This reduces the collective pitch of the blade thereby reducing the overall angle of the attack of the blade. The result is a more even distribution of the angle of attack throughout the blade which subsequently reduces the drag (Figs 8a,b). The minimal changes in the angle of attack

distribution in case of high speed cruise, between reference and optimum, partially explains the very small improvements obtained in η_c .

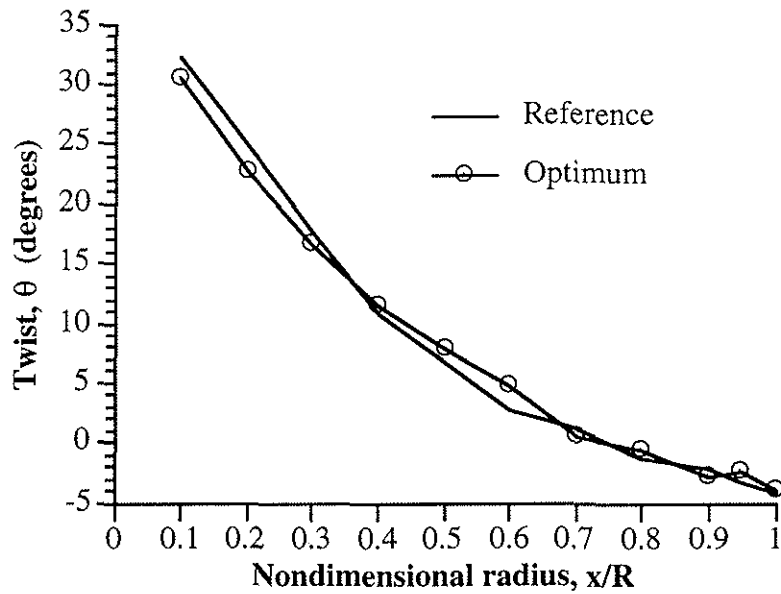


Figure 7 Blade twist distributions

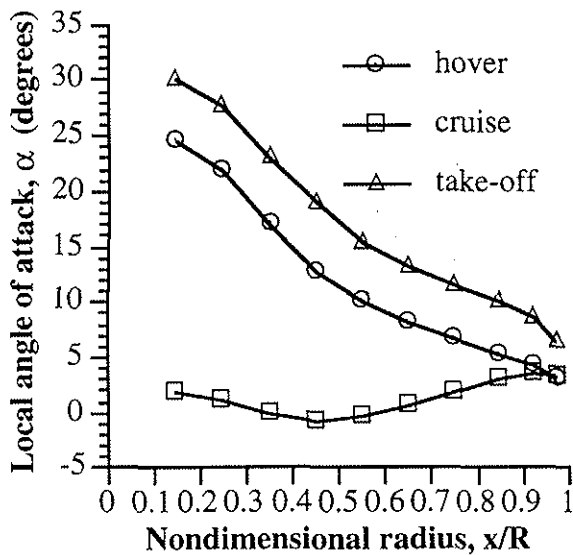


Figure 8a. Reference blade angle of attack

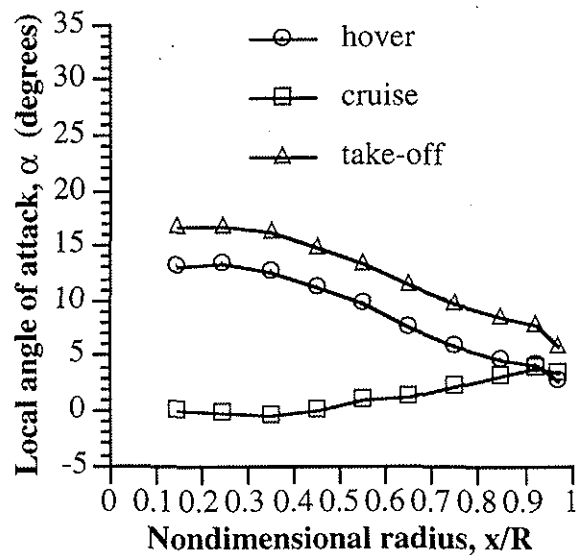


Figure 8b. Optimum blade angle of attack

Figure 9 shows the zero lift angle of attack distributions (α_{z1}) for both the reference and the optimum rotors. Significant decreases are observed from the reference values except at the tip. The result is an increase in airfoil camber which improves the lift-to-drag ratio thereby improving performance. However, associated with increased camber is higher drag divergence Mach numbers (M_{dd}) which can adversely affect the cruise performance. Therefore to avoid large drag penalties caused by operating the blade at local Mach numbers above M_{dd} , the zero lift angle of attack is only slightly reduced at the tip.

The rotor planform remains unswept after optimization. This is explained as follows. Since only static loading is included in this study and no aeroelastic stability requirements are imposed, the sweep of the blade was constrained during optimization such that the rotor could only be swept backwards. However, backward sweep induces large nose down pitching

moments which increases the magnitude of the elastic twist which is used as an objective function and is minimized at each flight condition. As a result, the optimizer avoids sweeping the blades to remain in the feasible domain.

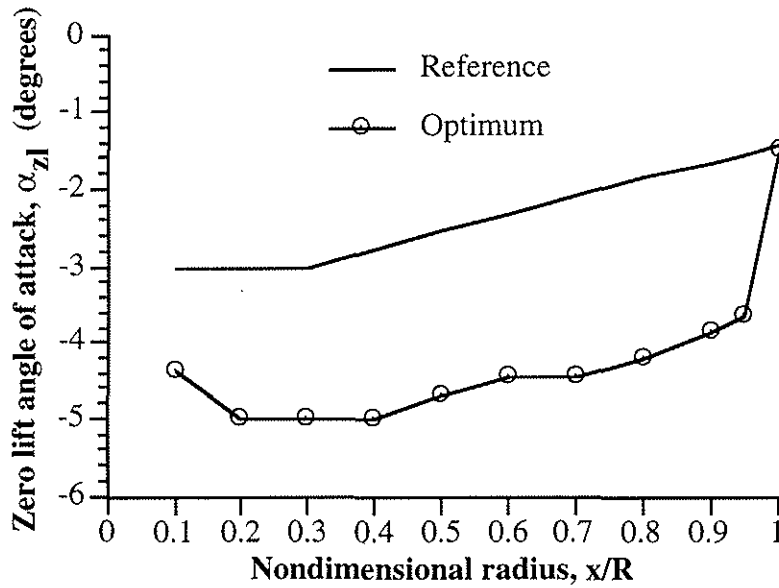


Figure 9 Zero lift angle of attack distributions

The lower level objective functions are presented in Table 3 and in Fig. 10 where large reductions from the reference rotor are observed in all six objective functions. The elastic twist in hover (ϕ_h), in cruise (ϕ_c) and in take-off (ϕ_t) are reduced by 14, 2.7 and 20 percent, respectively. The vertical displacement in hover (w_h) is reduced by 40 percent and in take-off (w_t) by 42 percent. The horizontal displacement in cruise (v_c) is reduced by 54 percent.

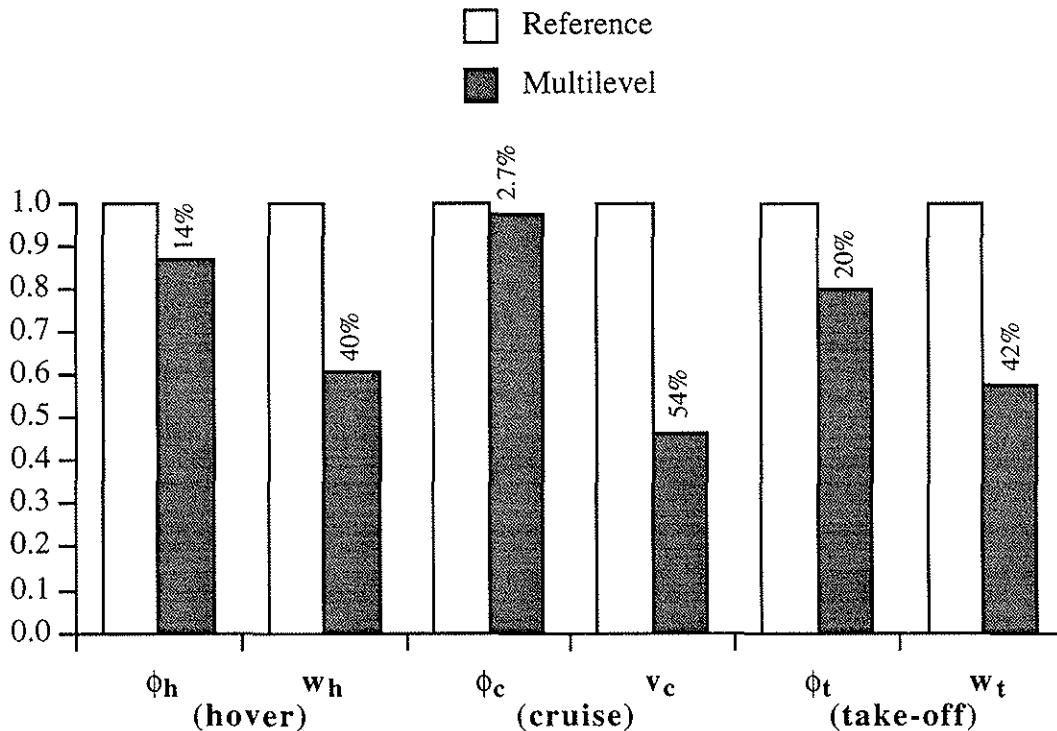


Figure 10 Summary of lower level objective functions

The composite laminate stacking sequences are presented in Table 4. Note that in the reference blade, the horizontal and vertical walls are assumed to have the same stacking sequence. Further, since all of the laminates are considered to be symmetric about their midplane, only 12 of the 24 total plies are presented in the table for each wall. The individual ply thickness used in this study is 0.001 in. which results in a total wall thickness of 0.24 in. The rearrangement of the stacking sequence after optimization represents a compromise between the conflicting requirements of reduced elastic twist and reduced transverse displacements. This is observed by noting the inclusion of ± 30 degree plies in both the horizontal and the vertical walls.

Table 4 Ply orientation angles

Reference		Optimum	
		Horizontal Wall	Vertical Wall
Outer ply	0°	15°	15°
	0°	-15°	-15°
	0°	0°	15°
	0°	0°	-15°
	15°	45°	30°
	-15°	-45°	-30°
	15°	45°	30°
	-15°	-45°	-30°
	45°	0°	0°
	-45°	0°	0°
	45°	30°	15°
	midplane	-45°	-30°

The displacement distributions of the reference and optimum rotors are presented in Figs. 11-14. Figure 11 shows the elastic twist (ϕ) distributions which are reduced in magnitude, after optimization, throughout the blade span in all three flight conditions. Note that the elastic twist values are all negative resulting in a nose down motion. Similar trends are observed in case of the transverse vertical displacement (Fig. 12), the transverse horizontal displacement (Fig. 13) and the axial displacement (Fig. 14). Since the centrifugal force is the only axial force acting on the blade which remains unchanged between reference and optimum, in both hover and during take-off, the axial deflections in both of these flight conditions remain the same. The reductions in all of the displacement distributions are attributable to the improved ply stacking sequence and the increased thickness of the airfoil due to larger chords which in turn increases the box beam height.

8. CONCLUDING REMARKS

A multiple design point optimization procedure was developed for the design of high speed propellers. A multilevel decomposition optimization technique was used to decompose the problem into two levels. Aerodynamic performance was the objective of the upper level and the structural response was improved at the lower level. Optimization was performed simultaneously to include high speed cruise, hover and take-off. The Kreisselmeier-Steinhauser function was used to formulate the multiple objective optimization problems at each level. At the upper level, a nonlinear programming technique based on the Broyden-Fletcher-Goldfarb-Shanno method was used as the optimization algorithm. A simulated annealing algorithm was used for the discrete optimization problem at the lower level. A total of 5 global cycles were required for convergence. The optimum results were compared with a reference rotor. Following are some important observations.

1. The multilevel optimization procedure significantly improves the aerodynamic and structural response of the high speed propeller blade at all three flight conditions.

2. The chord distribution of the optimum rotor closely resembles the ideal hover chord distribution. Exceptions are noted at the root and at the tip where the optimizer is driven by the geometric constraints imposed on the problem.
3. The airfoil thickness to chord ratio is significantly decreased at inboard section of the blade after optimization. This reduces the profile drag over this portion of the blade which improves the performance.
4. The optimum twist is reduced at inboard sections, increased over the mid section and remains largely unchanged at outboard sections. The result is a more optimum distribution of the local angle of attack which improves performance in hover and in take-off. The tip twist remains unchanged to maintain efficiency in high speed cruise.
5. The airfoil camber of the optimum blade is significantly increased from reference values to improve the airfoil lift-to-drag ratio resulting in increased aerodynamic efficiency.
6. The simulated annealing algorithm successfully minimizes the tip displacements by altering the composite plate stacking sequences in the horizontal and vertical walls. The optimum composite stacking sequence represents a compromise between reduced elastic twist and reduced transverse deformation. This is manifested through the selection of ± 30 degree plies in both the horizontal and the vertical walls.
7. A combination of improved stacking sequence and larger chord values leads to reduced elastic deformation in the optimum configurations.

9. ACKNOWLEDGMENTS

The authors acknowledge the support of this research through a grant from NASA Ames Research Center, Grant number NCC2-7995, Technical monitors, Mr. John F. Madden, III and Dr. Sesi Kottapalli.

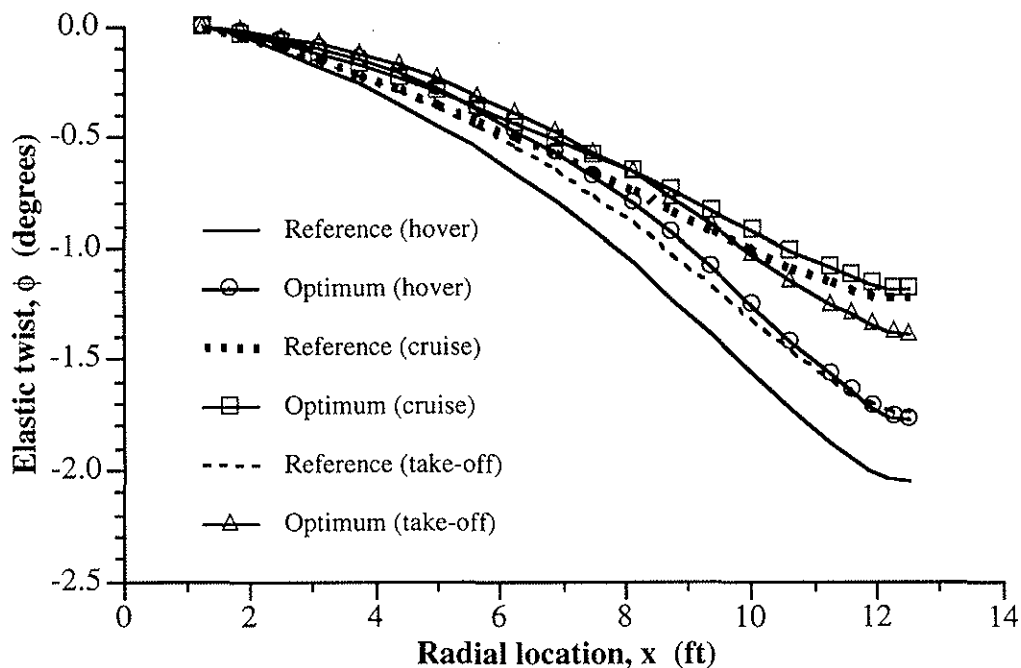


Figure 11 Elastic twist distributions

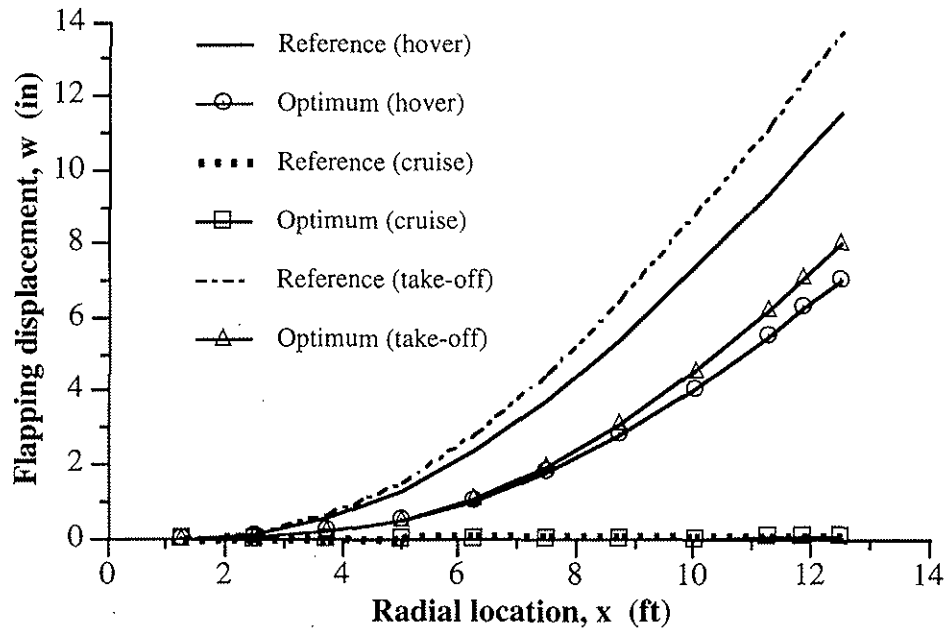


Figure 12 Transverse vertical displacement distributions

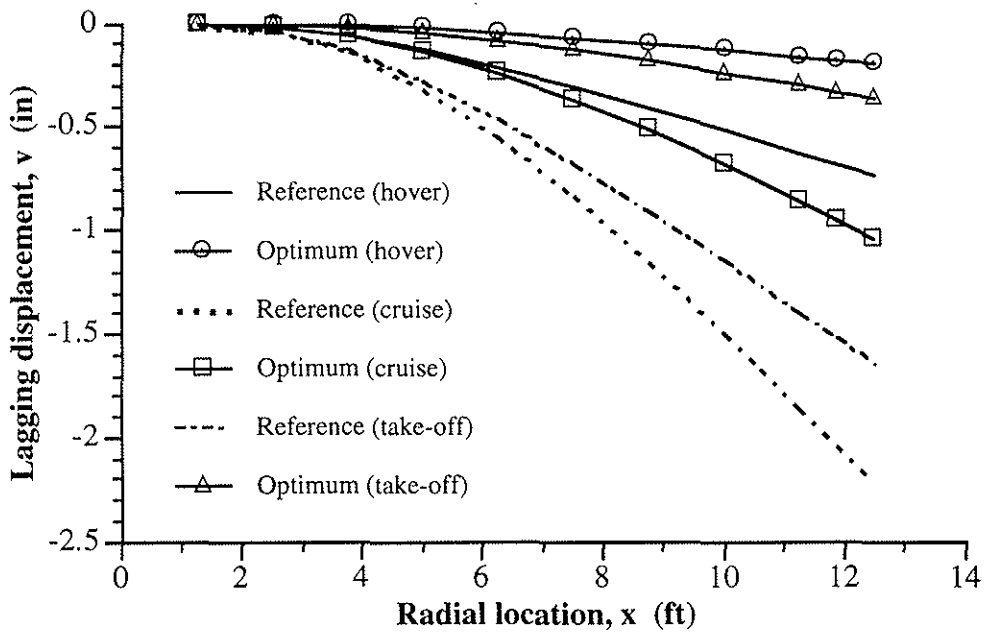


Figure 13 Transverse horizontal displacement distributions

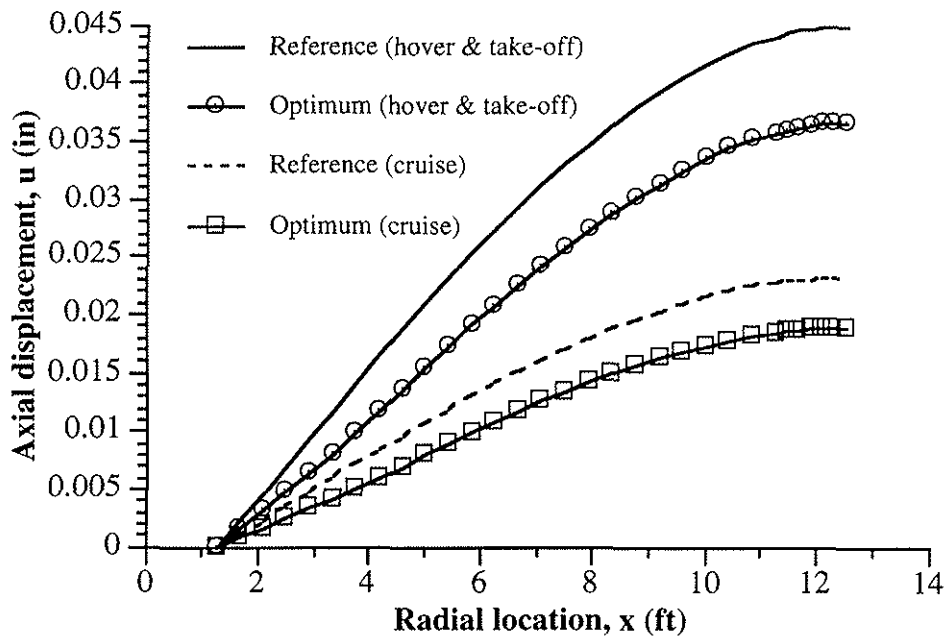


Figure 14 Axial displacement distributions

10. REFERENCES

1. Talbot, P., Phillips, J. and Totah, J., "Selected Design Issues of Some High Speed Rotorcraft Concepts," presented at the AIAA/AHS/ASEE Aircraft Design, Systems and Operations Conference, September 17 - 19, 1990, Dayton, Ohio.
2. Rutherford, J., O'Rourke, M., Martin, C., Lovenguth, M. and Mitchell, C., "Technology Needs for High speed Rotorcraft," NASA CR 177578, April 1991.
3. Wilkerson, J. B., Schneider, J. J. and Bartie, K. M., "Technology Needs for High speed Rotorcraft (1)," NASA CR 177585, May 1991.
4. Chattopadhyay, A. and Narayan, J., "Optimum Design of High Speed Prop-Rotors Using a Multidisciplinary Approach," presented at the 48th Annual Forum of the American Helicopter Society, June 3 - 5, 1992, Washington DC.
5. McCarthy, T. R. and Chattopadhyay, A., "Design of High Speed Proprotors Using Multiobjective Optimization Techniques," Paper No. AIAA 93-1032, *proc.* AIAA/AHS/ASEE Aerospace Design Conference, Irvine, California, February 16-19, 1993.
6. Chattopadhyay, A., McCarthy, T. R. and Madden, J. F., "Structural Optimization of High Speed Prop Rotors Including Aeroelastic Stability Constraints," *Mathematical and Computer Modelling*, Special Issue on Rotorcraft, Vol. 18, No. 3/4, pp. 101-113, 1993.
7. Chattopadhyay, A., McCarthy, T. R. and Madden, J. F., "A Design Optimization Procedure for Minimizing Drive System Weight of High Speed Prop-Rotors," *Engineering Optimization*, Vol. 23, No. 4 (in press). Also presented at the 4th AHS Rotorcraft Specialists Meeting on Multidisciplinary Design Optimization, Atlanta, Georgia, April 1993.
8. Chattopadhyay, A., McCarthy, T. R. and Madden, J. F., "An Optimization Procedure for the Design of Prop Rotors In High Speed Cruise Including the Coupling of Performance, Aeroelastic Stability and Structures" *Mathematical and Computer Modelling*, Special Issue on Rotorcraft, Vol. 19, No. 3/4, pp. 75-88, 1994. Also presented at the 49th Annual AHS Forum, St. Louis, Missouri, June 1993.

9. McCarthy, T.R., Chattopadhyay, A., Talbot, P.D., and Madden, J.F., "A Performance Based Optimization of High Speed Prop-Rotors," *Proc. of the American Helicopter Society Aeromechanics Specialists Conference*, San Francisco, January 1994.
10. Chattopadhyay, A., McCarthy, T. R. and Seeley, C. E., "A Decomposition Based Optimization Procedure for High Speed Prop-Rotors using Composite Tailoring and Simulated Annealing," *Proc. 50th Annual AHS Forum*, Washington, DC, May 1994.
11. Dadone, L., Liu, J., Wilkerson J. and Acree, C.W., "Proprotor Design Issues for High Speed Tiltrotors," *Proc. 50th Annual AHS Forum*, Washington, DC, May 1994.
12. Chattopadhyay, A. and Seeley, C. E., "A Simulated Annealing Technique for Multiobjective Optimization of Intelligent Structures," *J. Smart Mater. Struct.* **3**, 1994, pp. 98-106.
13. Lamon, S., "XV-15 Advanced Technology Blades, Ultimate Stress Analysis," Boeing Report Number D210-12345-1, 1985.
14. Smith, E.C. and Chopra, I., "Formulation and Evaluation of an Analytical Model For Composite Box-Beams," *Proc. 31st AIAA/AHS/ASME/ASCE/ASC SDM Conference*, Long Beach, CA, April 2-4, 1990.
15. Smith, R. L., "Closed Form Equations for the Lift, Drag, and Pitching-Moment Coefficients of Airfoil Sections in Subsonic Flow," NASA TM 78492
16. Talbot, P. D., "Propeller/Rotor Performance Code For Use in Preliminary Design," ATTT Project Office Working Paper FPT WP 001, NASA Ames Research Center, November 1993.
17. Glauert, H., The Elements of Aerofoil and Airscrew Theory, Cambridge University Press, Second Edition, 1948.
18. Walsh, J.L., Young, K. C, Pritchard, J.I., Adelman, H.M. and Mantay, W., "Multilevel Decomposition Approach to Integrated Aerodynamic/Dynamic/Structural Optimization of Helicopter Rotor Blades," *Proc. of the American Helicopter Society Aeromechanics Specialists Conference*, San Francisco, January 1994.
19. Chattopadhyay, A., McCarthy, T.R and Pagaldipti, N., "A Multilevel Decomposition Procedure for Efficient Design Optimization of Helicopter Rotor Blades," *Proc. 19th European Rotorcraft Forum*, Cernobbio, Italy, Paper n° G7, September 1993.
20. Tsai, S.W. and Wu, E.M., "A General Theory of Strength for Anisotropic Materials," *Journal of Composite Materials*, **5**, pp. 58-80, 1971.
21. Kreisselmeier, A. and Steinhauser, R., "Systematic Control Design by Optimizing a Vector Performance Index," *proc. of IFAC Symposium on Computer Aided Design of Control Systems*, Zurich, Switzerland, 1979, pp. 113-117.
22. Haftka, R. T., Gürdal, Z. and Kamat, M. P., Elements of Structural Optimization, Kluwer Academic Publishers, Dordrecht, The Netherlands, 1990.
23. Fadel, G. M., Riley, M. F. and Barthelemy, J. M., "Two Point Exponential Approximation Method for Structural Optimization," *Structural Optimization*, Vol. 2., pp. 117-224.
24. Thomas, H. L., Vanderplaats, G. N., Shyy, Y-K, "A Study of Move Limit Adjustment Strategies in the Approximation Concepts Approach to Structural Synthesis," *Proc. 4th AIAA/USAF/NASA/OAI Symposium on Multidisciplinary Analysis and Optimizations*, Cleveland, OH, September 1992. AIAA Paper No. 92-4750-CP.
25. Olsen, G. R. and Vanderplaats, G. N., "Method for Nonlinear Optimization with Discrete Design Variables," *AIAA Journal*, Vol. 27, No. 1, 15, November, 1989, pp. 1584-1589.